CONF-780314-3

LA-UR-78-1211

TITLE: PLANETARY GAMMA-RAY SPECTROSCOPY

AUTHOR(S): Robert C. Reedy

MASTER

SUBMITTED TO: 9th Lunar and Planetary Science Conference, Houston, TX, March 1978

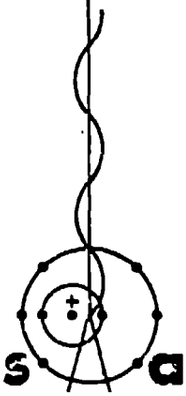

los alamos
scientific laboratory
of the University of California
LOS ALAMOS, NEW MEXICO 87545

Form No. 836 R2
St. No. 2629
1/78

DEPARTMENT OF ENERGY
CONTRACT W-7405-ENG. 36

PLANETARY GAMMA-RAY SPECTROSCOPY

by

Robert C. Reedy
Los Alamos Scientific Laboratory
Los Alamos, NM 87545

ABSTRACT

The chemical composition of a planet can be inferred from the gamma rays escaping from its surface and can be used to study its origin and evolution. The measured intensities of certain gamma rays of specific energies can be used to determine the abundances of a number of elements. The major sources of these gamma-ray lines are the decay of natural radionuclides, reactions induced by energetic galactic-cosmic-ray particles, capture of low-energy neutrons, and solar-proton-induced radioactivities. The fluxes of the more intense gamma-ray lines emitted from 30 elements were calculated using current nuclear data and existing models. The source strengths for neutron-capture reactions have been modified from those previously used. The fluxes emitted from a surface of average lunar composition are reported for 288 gamma-ray lines. These theoretical fluxes have been used elsewhere to convert the data from the Apollo gamma-ray spectrometers to elemental abundances and can be used with results from future missions to map the concentrations of a number of elements over a planet's surface. Detection sensitivities for these elements are examined and applications of gamma-ray spectroscopy for future orbiters to Mars and other solar-system objects are discussed.

20 April 1978

INTRODUCTION

Determining the chemical composition of a planet's surface is an essential part of the investigation of the planet. The abundances of certain elements with different condensation temperatures and with various types of geochemical behavior can provide valuable clues to a planet's origin and evolution (Anders, 1977). A planet's gross chemistry is established during its accretion from the solar nebula and certain elements are indicative of the nature of the early condensate, e.g., uranium (a refractory element in the early condensates), iron (condensed as metallic iron-nickel), and magnesium (the first silicate formed). Planetary processes, such as core and crust formation during differentiation and later magma formation and emplacement, greatly modify the distribution of the elements in the planet and produce the present crusted rocks. Geochemical clues to the evolution of a planet (Anders, 1977) include the supply of sulfur and metallic iron (formation of FeS), the ratio FeO/MnO (the oxidation of iron), the ratio K/U (remelting of the primordial condensates), and the ratio Tl/U (relative abundance of volatiles). Since many elements can be grouped according to their condensation and geochemical behavior, chemical abundance data for only a few key elements are needed to determine the origin and evolution of a planet.

The surface layers of a planet usually involve a regolith consisting of rock fragments and reworked materials, such as glasses. The extent to which regolith material has been transported away from its origin influences the chemistry of the surface layers of a planet. Transport mechanisms possible on various planets include meteoroid impact (ballistic or flow processes), water and wind movement, and electrostatically charged particles in electric

fields. The lateral movement of exotic material into geologically different provinces can be detected by photogeology or chemical analyses. Another source of foreign material is vertical mixing in regions with relatively thin layers of different composition. The composition of ejecta near a large crater often are different than that of the surface layer.

The chemical nature of a planetary surface can be determined from returned samples, by experimental instruments placed on the surface, or by remote-sensing experiments. Returned samples allow extensive analyses to be performed and surface instruments (on penetrators, rovers, or landers) can provide valuable data, but these results only apply to a localized region. Orbital experiments allow global surveys to be made of a planet's surface, and complement surface measurements (Haines et al., 1976).

Some orbital remote-sensing experiments, such as mass spectrometers and alpha-particle spectrometers, provide only a limited amount of information on surface chemistry. Measurements of the spectrum of albedo neutrons above a planet's surface can indicate the presence of hydrogen and the macroscopic properties for the transport of neutrons in the surface layers (Lingenfelter et al., 1961). The relative abundances of the major elements with atomic numbers up to about 20 can be measured by X-ray fluorscence, using solar X-rays as the exciting source (Haines et al., 1976). Successful X-ray fluorescence experiments were flown on Apollos 15 and 16 (Adler et al., 1973). Orbital X-ray fluorescence is only applicable to planets with no atmosphere because X-rays have very short mean free paths in matter. The relative reflectance in the wavelength region from 0.3 to 3.0 μm and absorption bands at certain wavelengths can be used to map several elements, such as titanium and iron, in several minerals. Earth-based multispectral measurements have been used to classify lunar regions on the basis of spectral type (McCord et

al., 1976). The physical properties of the regolith, such as soil maturity, also affect the reflectance spectrum. The above two techniques can map the distribution of a few elements in the very surface layers of a planet with good spatial resolution.

Gamma-ray lines emitted by various isotopes allow the abundances of many elements to be determined by gamma-ray spectroscopy. These gamma rays are produced in the top few tens of centimeters of the planet's surface and can be detected above planets with no or little atmosphere. The spatial resolution for an isotropic detector is fairly poor but can be improved by collimation (Haines et al., 1976). The flux of gamma-ray lines from a planetary surface is low, so long counting times over a given region are required, especially if collimation is used. These four geochemical mapping techniques generally complement each other, and their inclusion on future planetary polar orbiters will provide very valuable chemical data with which to study the planet's origin and evolution.

Gamma-Ray Spectroscopy

This paper discusses the applications of gamma-ray spectroscopy in mapping the distribution of certain elements in planetary surfaces. The fluxes of gamma-ray lines expected from the moon are given and used to examine the ability of orbital gamma-ray spectrometers to determine the concentrations of a number of elements in the surface of the moon, Mars, Mercury, asteroids, and comets.

Gamma-ray spectrometers were carried to the moon on Lunar 10 and Apollos 15 and 16 and to Mars on the Soviet Mars-5. The Apollo spectrometers allowed the relative variations of the natural radioelements (K, U, and Th) and certain other elements (such as Fe) to be mapped on a relatively fine scale over 20% of the lunar surface (Arnold et al., 1977). The abundances of Th,

K, Fe, Mg, and Ti were determined for a number of lunar regions overflown by the Apollo spectrometers by analyses of their gamma-ray spectra (Bielefeld et al., 1976).

The spectrometers flown on these missions used scintillator detectors made of NaI(Tl). Future planetary missions will probably use solid-state detectors of high-purity germanium, which allow greatly improved resolution of the detected gamma-ray lines (Metzger et al., 1975). Because of the poor resolution of NaI(Tl) detectors, only a few gamma-ray lines were actually observable in the Apollo lunar spectra. Since germanium detectors can distinguish between gamma-ray lines only a few keV in energy apart, they will detect many lines in the energy region of geochemical interest (0.2 to 10 MeV). To plan for such missions with high-resolution spectrometers, the fluxes expected for less intense gamma-ray lines (minor lines from major elements and major lines from minor elements) as well as those for strong lines must be calculated.

The fluxes of gamma-ray lines from the moon have been calculated by Gorenstein and Gursky (1970), Armstrong (1972), and Reedy et al. (1973). All three of these papers gave fluxes for only the strongest gamma-ray lines. This work is an extension of the calculations in Reedy et al. (1973), hereafter called RAT. It uses the same models as in RAT to determine source strengths for gamma-ray lines, although the absolute magnitude of the neutron-capture rate in the moon has been modified. The spatial resolution of an isotropic spectrometer is given in RAT and the effects of collimation on detection sensitivities are discussed in Metzger et al. (1975). The procedure for the data reduction of NaI(Tl) spectra presented in RAT has evolved to that described in Bielefeld et al. 1976).

The first spectral unfolding of the Apollo gamma-ray data (Metzger et al., 1974) used the lunar gamma-ray line fluxes of RAT. It was found that

the RAT library of fluxes was too small for good spectral unfolding (several lines unaccounted for and other lines poorly fitted), so a greatly expanded library of gamma-ray line fluxes was calculated. This improved library was used by Bielefeld et al. (1976) in unfolding the Apollo spectra and resulted in better fits to the lunar data. The gamma-ray line fluxes used by Bielefeld et al. (1976) are included here with only a few minor changes.

The major improvement in the gamma-ray line fluxes presented here is that more recent and better nuclear data was used in calculating the source strengths. In RAT, the energies of gamma-ray lines often were given only to the nearest 0.01 MeV and some lines several keV apart in energy were combined. Since germanium detectors have energy resolutions of several keV, the energies given here are as accurate as possible (usually to better than a keV) and only a very few lines with almost identical energies are combined. Many more gamma-ray lines were calculated for the major sources of lunar gamma rays (O, Mg, Al, Si, K, Ca, Ti, Fe, Th, and U) than those given in RAT. Also, gamma-ray line fluxes were calculated for 20 other elements, and any element likely to produce gamma-ray lines in planets, comets, or spacecraft was considered. The quality of the models used to calculate the fluxes and of the nuclear data (and hence of the calculated fluxes) is discussed. The fluxes are given for an average lunar chemical composition (Table I); RAT used the Apollo 11 soil chemistry. These calculated gamma-ray line fluxes are used to discuss the ability of orbital gamma-ray spectroscopy to determine elemental abundances on future planetary missions.

CALCULATED FLUXES

The general procedure used to calculate the flux of gamma-ray lines from a planetary surface is that described in RAT, and depends on the gamma-ray source strength as a function of depth and on the mass attenuation coefficient

for each gamma-ray energy. The calculated fluxes are for the photons which escape from a semi-infinite plane without undergoing any interactions. Four sources of gamma-ray lines are considered: decay of naturally occurring radionuclides, decay of solar-proton-induced radionuclides, reactions by energetic galactic-cosmic-ray (GCR) particles, and neutron-capture reactions. With a few exceptions, only gamma-ray lines with energies greater than about 0.2 MeV are considered here. For the major sources of lunar gamma-rays, the limit below which fluxes are not given was choosen so that this minimum flux was about the same for these elements at average lunar abundances.

Natural Radionuclides

The naturally occurring primordial radioactive nuclei (^{40}K, ^{138}La, ^{176}Lu, and the U and Th decay chains) were assumed to be uniformly distributed in the top few meters of the lunar surface. For each radionuclide, the half-life and the elemental atom abundance were 1.250×10^{9} y and 0.0001167 (^{40}K), 1.35×10^{11} y and 0.00089 (^{138}La), 3.6×10^{10} y and 0.026 (^{176}Lu), 1.40×10^{10} y and 1 (^{232}Th), and 7.04×10^{8} y, 0.0072 (^{235}U), and 4.47×10^{9} y and 0.9928 (^{238}U).

The parameters for ^{40}K, including the 0.1048 yield per ^{40}K disintegration for the 1.4608-MeV gamma-ray line from excited ^{40}Ar, are from Steiger and Jager (1977). The decay parameters for ^{138}La are from Pancholi and Martin (1976), and those for ^{176}Lu are from Horen and Harmatz (1976). Data for the 185.72 keV line of ^{235}U are from Schmorak (1977).

For gamma-ray lines produced by the daughters of ^{232}Th, recent measurements made by high-resolution gamma-ray spectrometers were evaluated to get energies and yields per disintegration of ^{232}Th. Beck (1972) reported absolute gamma-ray yields for the entire decay chain. Evaluated yields for the decay of ^{228}Ac were given by Horen (1976) and are adopted here. For the gamma rays emitted by the daughters of ^{228}Th, Heath (1974) and Avignone and

Schmidt (1978) reported relative yields (which were normalized assuming a yield of 0.307 for the 583.1 keV line produced by the decay of ^{208}Tl). The relative yields for the decay of ^{208}Tl presented by Pakkanen et al. (1969) and by Larsen and Jorgensen (1969) were normalized using a 0.360 yield for the 2.6146-MeV gamma ray. I evaluated these data to get the yields used for the daughters of ^{228}Th.

For the ^{238}U decay chain, the energies and yields in recent evaluations were adopted. All the gamma-ray lines with energies above 200 keV are emitted in the decay of ^{214}Pb and ^{214}Bi (Toth, 1977b). The 1.0010-MeV line emitted by the decay of ^{234m}Pa has only a 0.6% yield and was not included. The only other ^{238}U daughter emitting a relatively strong gamma ray is ^{226}Ra, which produces a gamma ray at 186.0 keV in its alpha-particle decay to ^{222}Rn (Toth, 1977a).

Table II gives the energy, yield, decaying nuclide, and flux escaping the moon for each of the gamma-ray lines emitted by natural radionuclides. For the ^{238}U and ^{232}Th decay chains, only lines with yields above about 1% are given. (Results are given to lower yields for high-energy gamma rays since they can travel farther in matter.) Most of the yields used here probably have uncertainties of ± 5% or less. Under the assumption of a source uniform with depth, the only other parameters involved in calculating the flux escaping the moon are the source strength (determined from the half-life of the radionuclide) and the mass attenuation coefficient, which both are known quite well. The overall uncertainties in the fluxes at gamma-rays from natural radionuclides are about ± 10%.

Solar-Proton-Induced Radioactivity

About 90% of the particles emitted from the sun during strong solar flares are protons and these protons travel only a few centimeters in the lunar surface before they are stopped by ionization energy losses (Reedy and

Arnold, 1972). Some of these solar protons induce low-energy reactions, producing several radionuclides which emit gamma-rays. Prompt gamma rays produced by solar protons will be extremely difficult to detect since the high proton flux incident on an actual detection system will saturate the spectrometer and charged-particle anti-coincidence circuits.

The lunar gamma-ray fluxes reported in RAT for solar-proton-induced radioactivities were for three different incident solar-proton spectral shapes (exponential-rigidity parameter, R_o, values of 50, 100, and 150 MV) and an omnidirection proton flux above 10 MeV of 100 protons/cm^2s. As discussed in Reedy and Arnold (1972), the activity of any given solar-proton-induced radionuclide at a given time depends on the solar-proton fluxes during the last few mean-lives of that nuclide. The gamma-ray fluxes reported here are those for solar-proton-induced radioactivities at the times of the Apollo 15 and Apollo 16 missions. The radionuclides considered are 7 x 10^5-year ^{26}Al, 2.6-year ^{22}Na, 303-day ^{54}Mn, and 78-day ^{56}Co; their activities were calculated using the model and cross sections of Reedy and Arnold (1972).

The activities of the short-lived radionuclides depend on the fluxe of solar protons since 1956. The evaluated solar-proton data of Reedy (1977) were used to calculate the activity-versus-depth profiles for ^{22}Na, ^{54}Mn, and ^{56}Co. For the Apollo 11, 12, and 14 missions, the agreements between calculated and observed profiles were quite good (Reedy, 1977). There are no depth-versus-activity profiles measured in samples from the Apollo 15 and 16 missions, so the profiles used to calculate gamma-ray fluxes were determined from the solar-proton fluxes of Reedy (1977). The solar-proton fluxes just before these missions were relatively low, so the induced ^{54}Mn and ^{56}Co activities were low and the uncertainties in their gamma-ray fluxes are large because the satellite solar-proton fluxes have not been confirmed by lunar

sample measurements. Most of the ^{22}Na activities during the Apollo 15 and 16 missions were made before Apollo 14 and 12, so the measured lunar rock data insures that the activity-versus-depth profiles used here are probably good to within about ± 20%.

The half-life of ^{26}Al is so long that contemporary solar-flare activity has a negligible effect on the lunar radioactivity-versus-depth profile. The ^{26}Al data in Apollo 12 and 14 rocks were used to derive the average solar-proton flux over its mean life of 80 protons/cm^{2}s above 10 MeV wi spectral shape of R_0 = 100 MV (Whalen et al., 1972). The uncertainties in this average flux and in the excitation functions used to calculate the expected activities for monoelemental targets result in an overall uncertainty for ^{26}Al gamma-ray fluxes of about ± 20%.

Table III gives the gamma-ray fluxes for these solar-proton-produced radioactivities at the times of the Apollo 15 and 16 missions. Because of its long half-life, the ^{26}Al values will be applicable to future lunar missions. The August 1972 solar flares produced much ^{22}Na, and more recent flares will produce additional atoms of ^{22}Na, ^{54}Mn, and ^{56}Co, so the fluxes of these and other short-lived radionuclides will need to be calculated from solar-proton measurements before future orbiter missions. If a strong solar flare occurs shortly before or during such a mission, activities of short-lived solar-proton-produced radionuclides, such as ^{56}Co and especially 16-day ^{48}V (made from titanium), will be very large, and their gamma-ray fluxes will be much larger than those reported here.

Solar-proton fluxes at other planets will vary depending on their distance from the sun (higher fluxes at Mercury, lower ones at Mars) and the positions of the planets in their orbit relative to the sun (since solar protons are not emitted isotropically from the sun, but travel out from the sun along specific magnetic field lines). Since solar protons are the least

important of the four gamma-ray sources reported here, the inability to predict solar-proton-induced radioactivity fluxes for other planets won't be a serious limitation. Relative ratios of gamma rays measured for radionuclides which are produced mainly from one target element, such as ^{48}V and ^{56}Co, could be used to study relative distributions of such elements, and the measured fluxes of other gamma-ray lines could be used to convert them to absolute values.

Energetic GCR Particle Reactions

The bombardment of the moon by the primary galactic cosmic rays (about 90% protons) produces many reactions and numerous secondary particles. Most secondary charged particles have low enough energies that they are stopped before they can induce a nuclear reaction, leaving neutrons as the major nuclear particle (Reedy and Arnold, 1972). Most of these secondary neutrons are produced with energies between 0.5 and 20 MeV, and can produce gamma-rays via nonelastic-scattering, $(n,x\gamma)$, reactions. High-energy GCR particles also can produce gamma-rays, denoted here as $(p,x\gamma)$ reactions, and some gamma-ray-emitting radionuclides. These secondary neutrons also can be slowed by scattering in the moon and captured via (n,γ) reactions. The production of gamma rays by neutron-capture reactions is discussed in the next section.

The model used for the fluxes of GCR particles as a function of depth in the moon was that of Reedy and Arnold (1972). For radionuclides at various depths in lunar samples, the ratios of the measured activities to the calculated production rates usually are ± 30% or less. No systematic trends in these ratios were observed either as a function of depth in the moon (including near the surface where gamma-ray production is most important) or of the effective energy of the nuclear reaction involved (low-energy reactions usually produce the strongest fluxes of gamma rays). As described in RAT, the source strengths for gamma rays produced by energetic GCR particles were

calculated using excitation functions for the relevant reactions and the Reedy-Arnold GCR fluxes. The sources and quality of the cross-section data are discussed below and the changes in the gamma-ray fluxes relative to those in RAT also are mentioned. A complete listing of references containing information on neutron reactions are given in CINDA (the Computer Index of Nuclear Data), issued periodically by the International Atomic Energy Agency, Vienna. Neutron reaction cross section data are compiled for many reactions in Garber and Kinsey (1976) and Bormann et al. (1974). For gamma-ray-production cross sections, the data measured at angles of about 55° or 125° with respect to the incident neutrons usually were used since these data are more typical of the values averaged over angle than those measured at other angles (such as 90°). Table IV gives the fluxes of gamma rays produced from the major elements (O, Mg, Al, Si, Ca, Ti, and Fe) by neutron nonelastic-scattering reactions and by the decay of GCR-produced radionuclides. The uncertainties given here should not be considered absolute, but are intended to indicate the relative quality of these fluxes.

The evaluated oxygen photon-production cross sections of Foster and Young (1972) and P. G. Young (private communication, 1975) were used for $(n,n\gamma)$, $(n,\alpha\gamma)$, and $(n,n\alpha\gamma)$ reactions. The cross sections used for the $^{16}O(n,p)^{16}N$ reaction were those in RAT. Relative to RAT, the gamma-ray fluxes from $(n,n\gamma)$ reactions are slightly lower, those from $(n,\alpha\gamma)$ reactions are up a factor of about 1.25, and that from the $(n,n\alpha\gamma)$ reaction up by 2.64. These new fluxes for oxygen gamma rays gave better fits to the Apollo data than those in RAT, especially for the $^{16}O(n,n\alpha\gamma)$ [illegible] 4.438 MeV (cf., Bielefeld et al., 1976). The quality of the evaluated cross section data for oxygen is quite good, comparable to some of those used for radionuclides, and I would estimate the uncertainties in these fluxes as of the order of ± 20%.

The quality of the magnesium cross-section data is poor, especially for gamma rays other than the one at 1.3686 MeV, since there have been few high-

resolution measurements made of Mg(n,xγ) reactions. The evaluated cross sections of Drake and Fricke (1975) and P. G. Young (private communication, 1975) were used for the 1.3686-MeV gamma ray. The flux calculated for this line is 1.07 of that in RAT. The gamma-ray lines produced by the decay of ^{24}Na were calculated using the same cross sections as in RAT, and that from ^{22}Na decay was calculated using the cross sections of Reedy and Arnold (1972). The uncertainties in the above magnesium gamma-ray fluxes are estimated to be about ± 25%. The (n,nγ) cross sections for other gamma rays from ^{24}Mg, ^{25}Mg, and ^{26}Mg were derived from various measurements below about 4.5 MeV and at 14-15 MeV. Their uncertainties are estimated to be of the order of ± 50%. Two gamma rays identified in NaI(Tl) spectra at about 6.2 and 7.2 MeV were not included here because of the uncertainties in their energies and because their fluxes are lower than those of the others reported here.

For aluminum (n,xγ) reactions, the evaluated cross sections of P. G. Young (private communication, 1975), based mainly on the measurements of Orphan and Hoot (1971), were used. The cross sections for ^{26}Al and ^{22}Na production were those of Reedy and Arnold (1972). The measurements of Bayhurst et al. (1975) were used for the ^{27}Al(n,α)^{24}Na reaction and the evaluated data of Young and Foster (1972) were adopted for the ^{27}Al(n,p)^{27}Mg reaction. The calculated gamma-ray fluxes are similar to those in RAT and their estimated uncertainties are about ± 25%.

The strongest silicon gamma-ray line is that at 1.7788 MeV via the ^{28}Si(n,nγ) reaction, and the measured cross sections of Dickens and Morgan (1974) and the evaluated ones of P. G. Young (private communication, 1975) were used. The cross sections used for other (n,xγ) reactions were based on the measurements of Dickens (1970) from 5.3 to 9.0 MeV, various other measurements, and evaluations of P. G. Young (private communication, 1975). The fluxes of the two strongest (n,nγ) gamma rays are 1.22 times greater than

those in RAT. The same cross sections as were used for RAT were used for the production of ^{22}Na, ^{24}Na, and ^{26}Al. The evaluated cross sections of Bhat et al. (1973) were used for the $^{28}Si(n,p)^{28}Al$ reaction. The gamma-ray fluxes from the decay of these radionuclides are identical or very similar to those of RAT. The uncertainties in the fluxes for silicon gamma rays are estimated to be of the order of ± 30%, although that for the 1.7788-MeV gamma ray probably is less.

The calcium cross-section measurements of Dickens (1972) and Dickens et al. (1974) were used for the gamma rays at 3.7366 and 3.9044 MeV from $^{40}Ca(n,n\gamma)$ reactions and that at 0.7705 MeV from the $^{40}Ca(n,p\gamma)$ reaction. Cross sections for other $Ca(n,x\gamma)$ reactions were based on the measurements of Dickens (1972) and miscellaneous other workers. The $^{40}Ca(n,n\gamma)$ fluxes are about factors of 1.3 greater than those in RAT. The estimated uncertainties in these gamma-ray fluxes are about ± 40%.

The measured titanium gamma-ray-production cross sections of Dickens (1974) for 4.9-, 5.4-, and 5.9-MeV neutrons were used and extended to and beyond various measurements at about 14.5 MeV. For the production of ^{46}Sc, various measured cross sections for the $^{46}Ti(n,p)$ and $^{47}Ti(n,np)$ reactions (cf., Garber and Kinsey, 1976) and estimated cross sections for the $^{48}Ti(n,x)^{46}Sc$ reaction were used. The flux of the 0.9834-MeV gamma ray reported in RAT was based only on estimated cross sections and was a factor of 1.85 lower than that calculated here. Because of the scarcity of measured cross sections for the $Ti(n,x\gamma)$ and $^{48}Ti(n,x)^{46}Sc$ reactions, the gamma-ray fluxes reported here probably have uncertainties of the order of ± 50%.

The $Fe(n,n\gamma)$ cross sections used were those of Orphan et al. (1975) and the cross sections for the production of ^{54}Mn were those of Reedy and Arnold (1972). The gamma-ray fluxes calculated here for these sources were very similar to those in RAT and their estimated uncertainties probably are about

± 25%. For gamma rays produced by $^{56}Fe(n,2n\gamma)$ reactions, the cross sections of Korkal'chuk et al. (1975) were used and their uncertainties are estimated to be of the order of ± 40%.

Table V gives the fluxes of gamma rays produced from 16 other elements by neutron nonelastic-scattering reactions or by the decay of GCR-produced radionuclides. Generally these gamma rays will not be detectable for small regions of a planet's surface, although some could be (such as nickel and sulfur on asteroids of chondritic compositions or carbon in comets). Some of these gamma rays will be detectable with long counting times for large regions of a planet (e.g., sodium, chromium, and manganese). The quality of the cross-section data is quite variable, ranging for different elements from very good to virtually non-existent.

The cross-section data for the $^{12}C(n,n\gamma)$ reaction producing the 4.4383-MeV gamma ray (Rogers et al., 1975) are very good, agreeing well with other measurements, and the flux uncertainty is about ± 20%. The cross-section data for $^{14}N(n,x\gamma)$ reactions of Rogers et al. (1975) are also of good quality and result in flux uncertainties of about ± 30%. The quality of the data of Morgan and Dickens (1976) for the 0.1971-MeV inelastic-scattering gamma ray of ^{19}F are about as good as those for nitrogen, while those for other prompt fluorine gamma rays are very poor, resulting in large uncertainties (of the order of ± 100%) in their gamma-ray fluxes. The cross sections used for $^{23}Na(n,n\gamma)$ reactions are based mainly on the measurements of Donati et al. (1977) and Dickens (1973), plus various ones near 14.5 MeV. The data for the $^{23}Na(n,2n)^{22}Na$ and $^{23}Na(n,\alpha)^{20}F$ are from Reedy and Arnold (1972) and from various sources (cf., Garber and Kinsey, 1976), respectively. The estimated uncertainties in the sodium gamma-ray fluxes are about ± 30%.

Kellie et al. (1973) was used for the $^{31}P(n,n\gamma)$ reactions and, since their data for iron agreed well with those adopted here, the data are probably

of reasonably good quality (about ± 40% uncertainty). The data for the $^{32}S(n,n\gamma)$ reaction producing the 2.2301-MeV gamma ray are of poor quality (uncertainty of over ± 50%) and probably include cross sections for gamma rays produced by the decay of the 4.47-MeV level to the 2.23-MeV level of ^{32}S. The gamma-ray fluxes for ^{35}Cl, ^{40}Ar, and ^{39}K are based only on a few measured cross sections and are of poor quality.

The scatter in the measured $^{52}Cr(n,n\gamma)$ and $^{55}Mn(n,n\gamma)$ cross sections is fairly large, and the resulting prompt gamma-ray fluxes are of poor quality. The evaluated data of Magurno amd Takahashi (1975) for the $^{55}Mn(n,2n)^{54}Mn$ reaction is of fairly good quality. The data for the inelastic-scattering reactions with ^{58}Ni and ^{60}Ni from many sources are of good quality, and those for the $^{58}Ni(n,p)^{58}Co$ reactions are also very good.

For the $^{88}Sr(n,n\gamma)$ reaction, I know of only one cross section (at 14.4 MeV), so the uncertainty in its flux is large. There is a fair amount of spread in the data which exist for the $^{89}Y(n,n\gamma)$ reactions, and there are no measurements between 5 and 14 MeV. The $^{89}Y(n,2n)^{88}Y$ and $^{90}Zr(n,2n)^{89}Zr$ cross sections of Bayhurst et al. (1975) are of very good quality, but the decay of these products produce gamma rays from levels in ^{88}Sr and ^{89}Y, respectively, so these particular gamma rays are less suitable for geochemical mapping because they usually will originate from reactions with two different elements. The data for the $^{90}Zr(n,n\gamma)$ gamma ray is of good quality, but the inelastic-scattering cross sections for the ^{92}Zr and ^{94}Zr nuclei are poorly known, being assumed equal to half of the measured values for 0.92-MeV gamma rays from natural zirconium. There exist no cross section data above 1.73 MeV for the $^{138}Ba(n,n\gamma)$ reaction, and the quality of the calculated gamma-ray flux is very poor. This 1.4359-MeV gamma ray is also made by the decay of the natural radionuclide ^{138}La.

Table VI gives fluxes of gamma rays produced by several high-energy reactions induced by GCR particles. The energies required to induce these spallation reactions are considerably above those for the (n,xγ) reactions considered above because several nucleons or alpha particles are removed from the target nucleus by these reactions. These reactions are denoted here as (p,xγ) since protons are more numerous than neutrons at these incident particle energies. These spallation reactions were not considered in RAT as a source of lunar gamma rays. A gamma-ray line in the Apollo spectra at 1.63 MeV can be explained and its flux reasonably well calculated by (p,xγ) reactions with Mg, Al, and Si producing the 1.6337 MeV excited level ^{20}Ne (cf., Bielefeld et al., 1976). The measurements of Foley et al. (1962), Chang et al. (1974), and Artun et al. (1975) for the bombardment of various targets with energetic protons show many (p,xγ) gamma rays. Their observations indicate that these reactions produce relatively strong fluxes of gamma rays from the de-excitation of the first level of 4n nuclei with even numbers of protons and neutrons and that most of these strong gamma rays are from product nuclei which are equivalent to the target nucleus minus one to three alpha particles.

In addition to the production of the ^{20}Ne line at 1.6337 MeV, other strong spallation lines observed include 2.6133 MeV (^{20}Ne), 1.3686 MeV (^{24}Mg from Al and Si), 2.2104 and 1.0144 MeV (^{27}Al from Si), 1.9704 (^{36}Ar from Ca), and 1.4342 MeV (^{52}Cr from Fe). The ^{20}Ne line at 2.6133 MeV will interfere with the detection of the thorium line at 2.6146 MeV. The only cross sections measured for this line were those of Foley et al. (1962), and result in fairly high calculated lunar gamma-ray fluxes (equivalent to about 0.4 ppm of thorium in the moon). The lunar gamma-ray data indicate that the flux of the 2.613-MeV line of ^{20}Ne is considerably lower than calculated (A. E. Metzger, private communication, 1977). The Foley et al. (1962) cross section for the

production of this line from magnesium is greater than that for the 1.634-MeV line of ^{20}Ne, which is inconsistent since, in ^{20}Ne, a 1.634-MeV gamma ray is always emitted after a 2.613-MeV gamma ray. For these reasons, the Foley et al. (1962) data for the 2.613-MeV line of ^{20}Ne were not used.

The scarcity of measured $(p,x\gamma)$ cross sections and the possible uncertainties in the few measured data result in poor quality gamma-ray fluxes. These spallation gamma rays generally are not suitable for elemental determinations, but are given here as examples of interferences which can occur in planetary gamma-ray spectra. The production of the 1.3686-MeV gamma-ray of ^{24}Mg by reactions with aluminum and silicon must be considered in determining magnesium abundances from this line, otherwise there will be an offset in these determined abundances. The low "ground truth" factors for magnesium of Bielefeld et al. (1976) could result from the presence of such spallation lines, although hopefully most of these $(p,x\gamma)$ lines were removed in the data analysis.

Neutron Capture

Many of the neutrons in the lunar surface have energies below the thresholds for nonelastic-scattering reactions (i.e., below about 0.5 MeV), and, as these low-energy neutrons travel through the lunar surface, they scatter from nuclei until they either escape from the surface or are captured by a nucleus. Many gamma rays, including some with high energies, are produced by such neutron-capture reactions. The spectra of these low-energy neutrons in the moon and their capture rates were calculated as a function of chemical composition by Lingenfelter et al. (1972), hereafter called LCH. The various effects of chemical composition on neutron-capture gamma-ray fluxes are discussed in RAT.

The total neutron-capture rates used in RAT were based on computer printouts provided by R. E. Lingenfelter and E. H. Canfield (private communication,

1971) for the rate for the capture of neutrons with energies below 3 eV. The factor used in RAT to convert this rate to the total neutron-capture rate was 1.77. This factor included nonelastic-scattering reactions in addition to (n,γ) reactions, and so resulted in an overestimation of the rates of lunar (n,γ) reactions. Detailed neutron fluxes in the moon as a function of depth and energy were provided by E. H. Canfield (private communication, 1973). Using neutron-capture cross sections which were inversely proportional to the neutron velocity ("1/v" cross sections) and these calculated neutron fluxes at a lunar depth of 4 g/cm^2, the ratio of the total "1/v" capture rate to that for neutrons with energies below 3 eV was determined to be 1.31, which is 0.74 of the factor used in RAT.

The best measurement of the neutron density in the moon was made by the Apollo 17 Lunar Neutron Probe Experiment -LNPE- (Woolum and Burnett, 1974, and Woolum et al. 1975). From tracks produced by the $^{10}B(n,\gamma)$ and $^{235}U(n,f)$ reactions, the lunar fluxes of low-energy neutrons were determined and compared with the theoretical fluxes of LCH. Woolum et al. (1975) concluded that the actual lunar neutron density was 0.8 of that used by LCH.

To convert the Apollo 17 LNPE results to a solar-cycle average, Woolum and Burnett (1974) derived a solar-cycle correction factor based on neutron fluxes measured in the Earth's atmosphere and on neutron-monitor counting rates. Since the neutron-monitor counting rate was greater at the time of the Apollo 17 mission than that averaged over a solar cycle, the Apollo 17 flux of neutrons was estimated to be a factor of 1.21 greater than the average flux of neutrons (Woolum and Burnett, 1974). Using this neutron-monitor approach, I determined solar-cycle correction factors for the Apollo 15 and 16 missions of about 1.15 and 1.19, respectively. A factor of 1.17 was adopted for the increase in the lunar neutron fluxes observed by the Apollo Gamma Ray Spectrometer Experiment relative to the solar-cycle-averaged flux.

The lunar neutron-capture gamma-ray fluxes calculated here are those applicable at the times of the Apollo experiments. These fluxes will need to be modified for future missions using solar-cycle correction factors determined during those missions. To convert RAT neutron-capture gamma-ray fluxes to those relevant for the Apollo experiments, the above three factors (0.74, 0.8, 1.17) must be multiplied to get the final conversion factor, 0.69.

Because the neutron fluxes at the times of the Apollo 15, 16, and 17 missions were very similar, the Apollo 17 LNPE neutron-capture rates can be used directly to determine a correction factor for those used in RAT. At a lunar depth of 150 g/cm^2, the measured ^{10}B capture rate in the LNPE (Woolum et al. 1975) was 467 ± 74 captures/s g(^{10}B) and that calculated by the capture rates used in RAT was 719. Thus the LNPE neutron-capture rates were 0.65 ± 0.10 of those used in RAT. The average of this factor and the 0.69 factor calculated above (0.67) was adopted to convert the neutron-capture rates used in RAT to those applicable to the Apollo gamma-ray data. Some of the neutron-capture rates used in these calculations (in units of captures/g s) for various lunar depths (in units of g/cm^2) were (0.00131,0), (0.00255,5), (0.00367,10), (0.00579,20), (0.00962,40), and (0.01437,70). The fraction of the neutrons captured by each element is given in Table I.

The neutron-capture gamma-ray fluxes reported in RAT were those calculated for the chemical composition of the Apollo 11 soil. This composition is fairly atypical of the average lunar composition given in Table I. The effective 1/v cross section for a given composition is $\Sigma_{eff} = N_o \Sigma(f_i\sigma_i/A_i)$, where N_o is Avogadro's Number, f_i is the weight fraction of element i, A_i is its atomic weight, σ_i is its effective 1/v capture cross section (cf., LCH; for major elements, σ_i is just its thermal cross section), and the sum is over all elements. For the average lunar and the Apollo 11 chemical compositions, the Σ_{eff} values are about 0.0066 and 0.0098 cm^2/g, respectively.

The neutron-capture gamma-ray fluxes for a given element vary with Σ_{eff}, the ratio of the fluxes for a given chemical composition to those for the average lunar composition being denoted the "chemical correction factor" (CCF). For 1/v - capturing nuclides, CCF is 0.01237 $(\Sigma_{eff})^{-0.876}$. Chemical correction factors calculated with this formula give values very similar to those given in RAT for several chemistries. A CCF factor of 1.40 should be used to convert the neutron-capture fluxes for an Apollo 11 chemistry to those for an average lunar chemistry.

The flux of a neutron-capture gamma ray for a given element depends on the gamma-ray's energy (which determines its mass attenuation coefficient), its yield per capture in that element, and the elemental neutron-capture rate. For all the elements reported here, the yields per capture were assumed to be those determined for the capture of thermal neutrons. The cross sections for the capture of thermal neutrons by these elements were taken from the evaluations of Mughabghab and Garber (1973). The capture cross section used for silicon in RAT was 10% higher than that used here. The yields per thermal capture were evaluated from literature data and the references used for my evaluations are cited below. Table VII gives the calculated fluxes of neutron-capture gamma rays produced by reactions with the major elements in the moon. The lowest fluxes given for each element were selected so that their values for an average lunar chemistry were about the same.

The magnesium neutron-capture yields of Spilling et al. (1967) are in very good agreement with other measurements. The aluminum measured yields of Nichol et al. (1969) and Ishag et al. (1972) were emphasized in determining the evaluated yields. The three sources mentioned in Bhat et al. (1973) for silicon were used in getting the yields. The calcium yields of Arnell et al. (1969) are the bases of the yields adopted here. For titanium, emphasis was placed on the yields of Tripathi et al. (1969). The iron yields used in RAT

were modified slightly using various other measurements. The agreement among the few measurements of iron's neutron-capture yields is good.

The quality of these neutron-capture yields for the major elements is quite good. Neutron-capture gamma rays mainly were used to determine iron and titanium abundances from the Apollo data and the ground truth factors for these elements in Bielefeld et al. (1976) varied about unity by only ± 20% or less. These ground truth factors indicate that the neutron-capture gamma-ray fluxes probably are accurate.

Table VIII gives neutron-capture gamma-ray fluxes for 15 other elements. The quality of the data for neutron-capture yields varied from very good to very poor, but only when the data is not good is there a comment. Neutron capture by hydrogen always results in a 2.2233-MeV gamma ray, the only gamma ray produced by hydrogen. Carbon, oxygen, and fluorine have very low (n,γ) cross sections and are not included here. The energies and neutron-capture yields given in Ajzenberg-Selove (1976) were used for ^{14}N. For sodium, the yields of Nichol et al. (1969) were emphasized in my evaluation. Phosphorus has a relatively low capture cross section and no gamma rays with high yields. The sulfur gamma-ray yields essentially were those of Egri et al. (1969). For chlorine, which has a high capture cross section, about six sources, cited in Spits and Kopecky (1976), were used to derive the yields adopted here. The yields for potassium were similar to those measured by Op den Kamp et al. (1972). There is only fair agreement among the yield data for chromium and nickel and various sources were used to get the yields used here. The yield data of Mellema and Postma (1970) were used for the prompt neutron-capture gamma rays of manganese. There are large spreads among the yields measured for strontium and yttrium. There is fairly good agreement among the reported yields for the capture gamma rays of neodymium and the decay gamma rays of ^{152g}Eu. The spreads among the yields given for samarium and gadolinium capture gamma rays were considerable.

DISCUSSION

These fluxes for gamma rays from the moon should include all the gamma rays likely to be seen on any future gamma-ray-spectroscopy mission to various planets, asteroids, or comets. Since the fluxes of nuclear particles in a spacecraft are similar to those used here, these gamma-ray fluxes can be used to estimate backgrounds from material in a spacecraft. The most intense gamma ray emitted from the moon for each element is given in Table I. Fig. 1 shows the fluxes of the lunar gamma rays as a function of energy.

An earlier version of this library of lunar gamma-ray fluxes, similar to the one given here, was used by Bielefeld et al. (1976) in unfolding the Apollo gamma-ray data. The only gamma-ray line in the Apollo spectra which was not fitted reasonably well by this library was one at about 2.2 MeV and it probably was produced via the capture of lunar-albedo neutrons by hydrogen in matter around the detector. Another preliminary version of this library was used by Metzger et al. (1975) in determining detection thresholds as a function of counting time for high-resolution detectors in orbit about the moon and Mars. Haines et al. (1976) discuss a large number of geochemical questions, such as the presence of volatiles at the lunar poles, which can be addressed by future gamma-ray-spectroscopy missions.

Several relatively strong gamma rays from different elements have energies similar enough that even a high-resolution detector could not resolve them. There are neutron-capture lines from Ca and Ti at energies of 6.420 and 6.419 MeV, respectively. The interference between the ^{208}Tl line at 2.6146 MeV and the (p,xγ) line of ^{20}Ne at 2.6133 MeV was mentioned above, but it should be a problem only for very low abundances (below 0.5 ppm) of thorium. Another example are the lines from Fe (0.8467), Al (0,8438), and Th (0.8402). Various gamma rays from the decay of uranium and thorium have energies close to those from other elements: e.g., 1.3777 MeV (U) and the ^{48}Ti(n,γ) line at

1.3815 MeV; 0.7684 (U), 0.7721 (Th), and the $^{40}Ca(n,p\gamma)$ line at 0.7705 MeV; and 1.2381 (U) and the $^{56}Fe(n,n\gamma)$ line at 1.2383 MeV.

In a number of cases, the same gamma-ray line can be produced by reactions with several different elements. Many of the $(p,x\gamma)$ reactions discussed above can produce gamma rays which also can be made by inelastic-scattering reactions. Such $(p,x\gamma)$ gamma rays will be a serious problem for minor elements whose major isotope is one to three "alpha particles" away from a major nuclide, e.g., the ^{32}S line at 2.2301 MeV made from ^{40}Ca and the ^{52}Cr line at 1.4342 being made from ^{56}Fe. Since the fluxes for the spallation gamma rays are not well determined, it will be hard to correct for the spallation contributions to these inelastic-scattering gamma rays for minor elements. A few radionuclides made from various elements will produce gamma rays which are also made by inelastic-scattering reactions in a different element. The decay of ^{24}Na (made readily from Al or Si) produces the 1.3686- and 2.7539-MeV gamma rays of ^{24}Mg.

The $^{16}O(n,n\alpha\gamma)$ reaction produces a strong flux of the 4.4383-MeV gamma ray from ^{12}C. An oxygen abundance of 5.83% produces the same flux of this gamma ray as a 1.00% abundance of carbon. Since oxygen is usually in most planetary surfaces with abundances of about 40 - 45%, the detection of carbon via this line will be difficult. Most of the excited levels in ^{12}C decay by the emission of three alpha particles. The level at 15.110 MeV is one of the few levels in ^{12}C which decays by gamma-ray emission, mainly decaying to the ground state. Cross sections for the production of this 15.110-MeV gamma ray have not been measured, so its flux can't be calculated. An other possible way to map carbon in a planet is to compare the flux of the 4.4383-MeV gamma ray with the fluxes for other oxygen gamma rays.

Mars is differert enough from the moon that the emission of gamma rays from its surface should be discussed. Metzger and Arnold (1970) discussed the general aspects of martian gamma-ray spectroscopy, including atmospheric

attenuation of gamma rays and spatial resolution. The presence of about 1% ^{40}Ar in the martian atmosphere will produce a flux of 1.4608-MeV gamma rays which is comparable to the flux from the decay of ^{40}K in approximately 100 ppm of K in the martian surface. Thus martian atmospheric argon will not seriously interfere with the detection of ^{40}K.

The presence of about 0.7% hydrogen in the martian surface would result in a neutron-capture chemical correction factor of approximately two (cf., discussion in RAT about the effects of hydrogen on neutron-capture gamma-ray fluxes); hence neutron-capture gamma-ray fluxes will be enhanced. If chlorine is present in the martian surface at the about 0.7% abundance reported by the Viking landers (Toulmin et al., 1977), its neutron-capture gamma rays will have fairly high fluxes. Similarly, the hydrogen line at 2.2233 MeV will be observable if the surface contains clay minerals like those used by Toulmin et al. (1977) to match the Viking lander chemical analyses or if it contains appreciable amounts of water.

Gamma-ray spectroscopy, especially from orbiters, is an excellent technique to map the distributions of a number of elements in a planetary surface. It is able to detect most major elements and several minor elements, including the natural radionuclides K, U, and Th, which are important sources of heat in a planetary interior. The spatial resolution possible with gamma-ray spectrometers is relatively poor, though more than adequate for the detailed study of a planet. Gamma rays can be used for the determination of elemental abundances in the moon, Mars, Mercury, asteroids, and comets. Hopefully, high-resolution gamma-ray spectrometers soon will be flown on missions to these interesting planets and solar-system objects.

ACKNOWLEDGMENTS

Discussions with the other members of the Apollo Gamma-Ray Spectrometer team, especially J. R. Arnold, A. E. Metzger, J. I. Trombka, and M. J. Bielefeld, have been very helpful in doing this work. I also wish to thank G. P. Russ III for explaining the details of the LCH neutron-flux calculations and P. G. Young for providing numerous tables and unpublished graphs containing evaluated photon-production cross sections. This work was performed under the auspices of the Department of Energy (DOE) and was supported by the National Aeronautics and Space Administration (NASA).

REFERENCES

Adler I., Trombka J. I., Lowman P., Schmadebeck R., Blodget H., Eller E., Yin L., Lamothe R., Osswald G., Gerard J., Gorenstein P., Bjorkholm P., Gursky H., Harris B., Arnold J., Metzger A.,and Reedy R. (1973) Apollo 15 and 16 results of the integrated geochemical experiment. The Moon 7, 487-504.

Ajzenberg-Selove F. (1976) Energy levels of light nuclei A = 13-15. Nucl. Phys. A268, 1-204.

Anders E. (1977) Chemical composition of the moon, Earth, and eucrite parent body. Phil. Trans. Roy. Soc. Lond. A285, 23-40.

Armstrong T. W. (1972) Calculation of the lunar photon albedo from galactic and solar proton bombardment. J. Geophys. Res. 77, 524-536.

Arnell S. E., Hardell R., Skeppstedt O., and Wallander E. (1969) Gamma rays from thermal neutron capture in ^{40}Ca, ^{42}Ca, ^{43}Ca, ^{44}Ca and ^{48}Ca. In Neutron Capture Gamma-Ray Spectroscopy, p. 231-255. International Atomic Energy Agency, Vienna.

Arnold J. R., Metzger A. E., and Reedy R. C. (1977) Computer-generated maps of lunar composition from gamma-ray data. Proc. Lunar Sci. Conf. 8th, p. 945-948.

Artun O., Cassagnon Y., Legrain R., Lisbona N., Roussel L., Alard J. P., Baldit A., Costilhes J. P., Fargeix J., Roche G., and Tamain J. C. (1975) Multinucleon removal induced by high-energy protons. Phys. Rev. Lett. 35, 773-775.

Avignone F. T. and Schmidt A. G. (1978) γ-ray and internal-conversion intensity studies of transitions in the decay of ^{228}Th. Phys. Rev. C 17, 380-384.

Bayhurst B. P., Gilmore J. S., Prestwood R. J., Wilhelmy J. B., Jarmie N., Erkkila B. H., and Hardekopf R. A. (1975) Cross sections for (n,xn) reactions between 7.5 and 28 MeV. Phys. Rev. C 12, 451-467.

Beck Harold L. (1972) Absolute intensities of gamma rays from the decay of ^{238}U and ^{232}Th. AEC report number HASL-262. 14 pp.

Bhat M. R., Goldberg M. D., Kinsey R. R., Prince A., and Takahashi H. (1973) Neutron and gamma ray production cross sections for silicon. AEC report BNL 50379. 52 pp.

Bielefeld M. J., Reedy R. C., Metzger A. E., Trombka J. I., and Arnold J. R. (1976) Surface chemistry of selected lunar regions. Proc. Lunar Sci. Conf. 7th, p. 2661-2676.

Bormann M., Neuert H., and Scobel W. (1974) Tables and graphs of cross-sections for (n,p), (n,α), and (n,2n) reactions in the neutron energy region 1 - 37 MeV. In Handbook on Nuclear Activation Cross-Sections, p. 87-272. International Atomic Energy Agency, Vienna.

Chang C. C., Wall N. S., and Fraenkel Z. (1974) Gamma rays observed from 100-MeV protons interacting with ^{56}Fe and ^{58}Ni. Phys. Rev. Lett. 33. 1493-1496.

Dickens J. K. (1970) $^{28\text{-}30}$Si(n,xγ) reactions for $5.3 \leq E_n \leq 9.0$ MeV. Phys. Rev. C 2, 990-1005.

Dickens J. K. (1972) Neutron induced gamma-ray reactions in calcium in the energy range $4.85 \leq E_n \leq 8.05$ MeV. Nucl. Sci. Eng. 48, 78-86.

Dickens J. K. (1973) The neutron-induced gamma-ray reactions in sodium-23 in the energy range $4.85 \leq E_n \leq 7.5$ MeV. Nucl. Sci. Eng. 50, 98-107.

Dickens J. K. (1974) Neutron-induced gamma-ray production in titanium for incident-neutron energies of 4.9, 5.4, and 5.9 MeV. Nucl. Sci Eng. 54, 191-196.

Dickens J. K., Love T. A., and Morgan G. L. (1974) Neutron-induced gamma-ray production in calcium in the energy range $0.7 \leq E_n \leq 20$ MeV. Nucl. Sci. Eng. 53, 277-284.

Dickens J. K. and Morgan G. L. (1974) ^{28}Si(n,n'γ) photon production cross sections for $E_\gamma = 1.78$ MeV, $5.0 \leq E_n \leq 9.5$ MeV. Phys. Rev. C 10, 958-960.

Donati D. R., Mathur S. C., Sheldon E., Barnes B. K., Beghian L. E., Harihar P., Kegel G. H. R., and Schier W. A. (1977) Cross sections, angular distributions, and magnetic substate populations in the ^{23}Na(n,n'γ) reaction. Phys. Rev. C

16, 939-957.

Drake M. K. and Fricke M. P. (1975) Evaluation of neutron and photon-production cross sections for natural magnesium. DNA report number DNA 3479F. 86 pp.

Egri Sh., Kardon B., Poch L., Sheresh Z., and Zamori Z. (1969) Spectrum of γ rays produced during thermal neutron capture by sulfur nuclei. Izv. Akad. Nauk SSSR, Ser. Fiz. 33, 1259-1262 (In Russian).

Foley K. J., Clegg A. B., and Salmon G. L. (1962) Gamma-radiation from the medium energy proton bombardment of sodium, magnesium, aluminium, silicon, phosphorus and sulfur. Nucl. Phys. 37, 23-44.

Foster D. G. and Young P. G. (1972) A preliminary evaluation of the neutron and photon-production cross sections of oxygen. AEC report LA-4780. 30 pp.

Garber D. I. and Kinsey R. R. (1976) Neutron cross sections volume II, curves. ERDA report number BNL 325, Third Edition, Volume II. 489 pp.

Gorenstein P. and Gursky H. (1970) Characteristic γ- and X-radiation in the planetary system. Space Sci. Rev. 10, 770-829.

Haines E. L., Arnold J. R., and Metzger A. E. (1976) Chemical mapping of planetary surfaces. IEEE Trans. Geosci. Electronics GE-14, 141-153.

Heath R. L. (1974) Gamma-Ray spectrum catalogue. AEC report number ANCR-1000-2. (numbered in sections).

Horen D. J. (1976) Nuclear data sheets for A = 228. Nucl. Data Sheets 17, 367-390.

Horen D. J. and Harmatz B. (1976) Nuclear data sheets for A = 176. Nucl. Data Sheets 19, 383-444.

Ishaq A. F. M., Colenbrander A. H., and Kennett T. J. (1972) Study of thermal neutron capture in aluminum. Can. J. Phys. 50, 2845-2855.

Kellie J. D., Islam M. N., and Crawford G. I. (1973) Inelastic neutron scattering by ^{56}Fe and ^{31}P in the energy range 0.8 to 9.0 MeV. Nucl. Phys. A208, 525-544.

Korkal'chuk V., Prokopets G. A., and Holmqvist B. (1975) Interaction of 16-22-MeV neutrons with iron nuclei. Sov. J. Nucl. Phys. 20, 574-578.

Larsen J. S. and Jorgensen B. C. (1969) The decay of ^{208}Tl. Gamma-ray measurement. Z. Physik 227, 65-70.

Lingenfelter R. E., Canfield E. H., and Hess W. N. (1961) The lunar neutron flux. J. Geophys. Res. 66, 2665-2671.

Lingenfelter R. E., Canfield E. H., and Hampel V. E. (1972) The lunar neutron flux revisited. Earth Planet. Sci. Lett. 16, 355-369.

Magurno B. A. and Takahashi H. (1975) Evaluation of the ^{55}Mn(n,2n) cross section for ENDF/B-IV. In ENDF/B-IV Dosimetry File (B. A. Magurno, Ed.), p. 70-79. Brookhaven National Laboratory, Upton.

McCord T. B., Pieters C., and Feierberg M. A.(1976) Multispectral mapping of the lunar surface using ground-based telescopes. Icarus 29, 1-34.

Mellema J. and Postma H. (1970) Investigation of nuclear level spins of ^{56}Mn by means of nuclear orientation. Nucl. Phys. A154, 385-406.

Metzger A. E. and Arnold J. R. (1970) Gamma ray spectroscopic measurements of Mars. Applied Optics 9, 1289-1303.

Metzger A. E., Trombka J. I., Reedy R. C., and Arnold J. R. (1974) Element concentrations from lunar orbital gamma-ray measurements. Proc. Lunar Sci. Conf. 5th, p. 1067-1078.

Metzger A. E., Parker R. H., Arnold J. R., Reedy R. C., and Trombka J. I. (1975) Preliminary design and performance of an advanced gamma-ray spectrometer for future orbiter missions. Proc. Lunar Sci. Conf. 6th, p. 2769-2784.

Morgan G. L. and Dickens J. K. (1976) Production of low-energy gamma rays by neutron interactions with fluorine for incident neutron energies between 0.1 and 20 MeV. Nucl. Sci. Eng. 60, 36-43.

Mughabghab S. F. and Garber D. I. (1973) Neutron cross sections volume I, resonance parameters. AEC report number BNL 325, Third Edition, Volume I. (paged in sections).

Nichol L. W., Colenbrander A. H., and Kennett T. J. (1969) A study of the $^{23}Na(n,\gamma)^{24}Na$ and $^{27}Al(n,\gamma)^{28}Al$ reactions. Can. J. Phys. 47, 953-961.

Op den Kamp A. M. F. and Spits A. M. J. (1972) Gamma rays from thermal-neutron capture in natural and ^{39}K enriched potassium. Nucl. Phys. A180, 569-586.

Orphan V. J. and Hoot C. G. (1971) Gamma-ray production cross sections for iron and aluminum. DNA 2736F (Gulf-RT-A10743) 199 pp.

Orphan V. J., Hoot C. G., and Rogers V. C. (1975) Gamma-ray production cross sections for iron from 0.86 to 16.7 MeV. Nucl. Sci. Eng. 57, 309-327.

Pakkanen A., Kantele J., and Suominen P. (1969) Levels in ^{208}Pb populated in the decay of ^{208}Tl(ThC"). Z. Physik 218, 273-281.

Pancholi S. C. and Martin M. J. (1976) Nuclear data sheets for A = 138. Nucl. Data Sheets 18, 167-222.

Reedy R. C. (1976) Solar proton fluxes since 1956. Proc. Lunar Sci. Conf. 8th, p. 825-839.

Reedy R. C. and Arnold J. R. (1972) Interaction of solar and galactic cosmic-ray particles with the moon. J. Geophys. Res. 77, 537-555.

Reedy R. C., Arnold J. R., and Trombka J. I. (1973) Expected γ ray emission spectra from the lunar surface as a function of chemical composition. J. Geophys. Res. 78, 5847-5866.

Rogers V. C., Orphan V. J., Hoot C. G., and Verbinski V. V. (1975) Gamma-ray production cross sections for carbon and nitrogen from threshold to 20.7 MeV. Nucl. Sci. Eng. 58, 298-313.

Schmorak M. R. (1977) Nuclear data sheets for A = 231, 235, 239. Nucl. Data Sheets 21, 91-200.

Spilling P., Gruppelaar H., and Op den Kamp A. M. F. (1967) Thermal-neutron capture gamma rays from natural magnesium and enriched ^{25}Mg. Nucl. Phys. A102, 209-225.

Spits A. M. J. and Kopecky J. (1976) The reaction $^{35}Cl(n,\gamma)^{36}Cl$ studied with non-polarized and polarized thermal neutrons. Nucl. Phys. A264, 63-92.

Steiger R. H. and Jager E. (1977) Subcommission on geochronology: convention on the use of decay constants in geo- and cosmochronology. Earth Planet. Sci. Lett. 36, 359-362.

Toth K. S. (1977a) Nuclear data sheets for A = 222. Nucl. Data Sheets 21, 479-492.

Toth K. S. (1977b) Nuclear data sheets for A = 214. Nucl. Data Sheets 21, 437-466.

Toulmin P., Baird A. K., Clark B. C., Keil K., Rose H. J., Christian R. P., Evans P. H., and Kelliher W. C. (1977) Geochemical and mineralogical interpretation of the Viking inorganic chemical results. J. Geophys. Res. 82, 4625-4634.

Tripathi K. C., Blichert-Toft P. H., and Boreving S. (1969) Thermal neutron capture gamma-ray studies of natural titanium. In Neutron Capture Gamma-Ray Spectroscopy, p. 183-198. International Atomic Energy Agency, Vienna.

Wahlen M., Honda M., Imamura M., Fruchter J. S., Finkel R. C., Kohl C. P., Arnold J. R., and Reedy R. C. (1972) Cosmogenic nuclides in football-sized rocks. Proc. Lunar Sci. Conf. 3rd, p. 1719-1732.

Woolum D. S. and Burnett D. S. (1974) In-situ measurement of the rate of ^{235}U fission induced by lunar neutrons. Earth Planet. Sci. Lett. 21, 153-164.

Woolum D. S., Burnett D. S., Furst M., and Weiss J. R. (1975) Measurement of the lunar neutron density profile. The Moon 12, 231-250.

Young P. G. and Foster D. G. (1972) A preliminary evaluation of the neutron and photon-production cross sections for aluminum. AEC report number LA-4726. 40 pp.

Table I

For each element considered here, its average abundance in the moon (as adopted for these calculations), the fraction of low-energy neutrons it captures, and its most intense gamma ray escaping from the moon.

Element	mg/g[a]	Fraction captured	Strongest lunar gamma ray		
			Source[b]	Energy (MeV)	photons/cm^2 min
H	0.04	0.0012	$^{1}H(n,\gamma)$	2.2233	0.00342
C	0.1[c]	---	$^{12}C(n,n\gamma)$	4.4383	0.00163
N	0.1[c]	---	$^{14}N(n,n\gamma)$	2.3127	0.000323
O	430.	---	$^{16}O(n,n\gamma)$	6.1294	2.562
F	0.1	---	$^{19}F(n,n\gamma)$	0.1971	0.00144
Na	3.5	0.0074	$^{23}Na(n,n\gamma)$	0.4399	0.0558
Mg	40.	0.0095	$^{24}Mg(n,n\gamma)$	1.3686	0.727
Al	110.	0.0857	$^{27}Al(n,n\gamma)$	2.2104	0.674
Si	200.	0.104	$^{28}Si(n,n\gamma)$	1.7788	3.223
P	0.6	0.0003	$^{31}P(n,n\gamma)$	1.2661	0.0038
S	0.7	0.0010	$^{32}S(n,n\gamma)$	2.2301	0.0067
Cl	0.02	0.0017	$^{35}Cl(n,\gamma)$	6.111	0.00211
K	1.2	0.0059	^{40}K	1.4608	2.342
Ar	0.1[c]	---	$^{40}Ar(n,n\gamma)$	1.4608	0.0013
Ca	100.	0.098	$^{40}Ca(n,n\gamma)$	3.7366	0.346
Ti	14.	0.163	$^{48}Ti(n,\gamma)$	6.7615	0.404
Cr	1.0	0.0055	$^{52}Cr(n,n\gamma)$	1.4342	0.0160
Mn	0.8	0.0177	^{56}Mn	0.8467	0.024
Fe	90.	0.376	$^{56}Fe(n,n\gamma)$	0.8467	1.149
Ni	0.4	0.023	$^{58}Ni(n,\gamma)$	8.999	0.0072

Table I, cont.

Element	mg/g[a]	Fraction captured	Strongest lunar gamma ray Source[b]	Energy (MeV)	photons/cm^2 min
Sr	0.18	0.0002	$^{88}Sr(n,n\gamma)$	1.8360	0.0019
Y	0.06	0.0001	$^{89}Y(n,n\gamma)$	1.5074	0.00024
Zr	0.25	---	$^{90}Zr(n,n\gamma)$	2.1865	0.00090
Ba	0.20	0.0002	$^{138}Ba(n,n\gamma)$	1.4359	0.00147
La	0.010	---	^{138}La	1.4359	0.00247
Nd	0.017	0.0005	$^{143}Nd(n,\gamma)$	0.697	0.00042
Sm	0.007	0.027	$^{149}Sm(n,\gamma)$	0.3340	0.014
Eu	0.0005	0.0011	^{152g}Eu	1.409	0.0024
Gd	0.008	0.071	$Gd(n,\gamma)$	1.187	0.014
Lu	0.0005	---	^{176}Lu	0.3069	0.00756
Th	0.0019	---	^{208}Tl	2.6146	2.193
U	0.0005	---	^{214}Bi	0.6093	1.118

[a]The abundance as mg of element per g of lunar surface material.

[b]The reaction or radionuclide producing the most intense gamma ray.

[c]Nominal abundance used in these calculations, not a lunar abundance.

Table II

The fluxes of gamma rays produced by the decay of the natural radionuclides at the lunar elemental abundances of Table I. The yield is per disintegration of the parent radionuclide.

Element	Nuclide	Energy (MeV)	Yield	Flux (Photons/cm^2 min)
K	^{40}K	1.4608	0.1048	2.342
La	^{138}La	1.4359	0.671	0.00247
	^{138}La	0.7887	0.329	0.00090
Lu	^{176}Lu	0.3069	0.94	0.00756
	^{176}Lu	0.2018	0.85	0.00573
Th	^{208}Tl	2.6146	0.360	2.193
	^{228}Ac	1.6304	0.020	0.0967
	^{212}Bi	1.6205	0.016	0.0771
	^{228}Ac	1.5879	0.037	0.177
	^{228}Ac	1.4592	0.010	0.0458
	^{228}Ac	0.9689	0.175	0.656
	^{228}Ac	0.9646	0.055	0.206
	^{228}Ac	0.9111	0.290	1.054
	^{208}Tl	0.8605	0.045	0.159
	^{228}Ac	0.8402	0.010	0.0349
	^{228}Ac	0.8356	0.018	0.0627
	^{228}Ac	0.7948	0.048	0.163
	^{212}Bi	0.7854	0.010	0.0338
	^{228}Ac	0.7721	0.016	0.0537
	^{228}Ac	0.7552	0.011	0.0366
	^{212}Bi	0.7272	0.070	0.229
	^{208}Tl	0.5831	0.307	0.916
	^{228}Ac	0.5623	0.010	0.0294
	^{208}Tl	0.5107	0.085	0.240
	^{228}Ac	0.4630	0.046	0.125
	^{228}Ac	0.4094	0.022	0.0566
	^{228}Ac	0.3384	0.120	0.285

Table II, cont.

Element	Nuclide	Energy (MeV)	Yield	Flux (Photons/cm^2 min)
Th	^{228}Ac	0.3280	0.034	0.0798
	^{212}Pb	0.3000	0.031	0.0700
	^{208}Tl	0.2774	0.024	0.0524
	^{228}Ac	0.2703	0.038	0.0821
	^{224}Ra	0.2410	0.038	0.0783
	^{212}Pb	0.2386	0.47	0.964
	^{228}Ac	0.2094	0.045	0.0874
U	^{214}Bi	2.4477	0.016	0.0753
	^{214}Bi	2.2041	0.050	0.224
	^{214}Bi	2.1185	0.012	0.0526
	^{214}Bi	1.8474	0.021	0.0861
	^{214}Bi	1.7645	0.159	0.637
	^{214}Bi	1.7296	0.031	0.123
	^{214}Bi	1.6613	0.0115	0.0448
	^{214}Bi	1.5092	0.022	0.0817
	^{214}Bi	1.4080	0.025	0.0897
	^{214}Bi	1.4015	0.014	0.0501
	^{214}Bi	1.3777	0.040	0.142
	^{214}Bi	1.2810	0.015	0.0514
	^{214}Bi	1.2381	0.059	0.199
	^{214}Bi	1.1552	0.017	0.0554
	^{214}Bi	1.1203	0.150	0.481
	^{214}Bi	0.9341	0.032	0.0939
	^{214}Bi	0.8062	0.012	0.0328
	^{214}Pb	0.7859	0.011	0.0297
	^{214}Bi	0.7684	0.049	0.131
	^{214}Bi	0.6555	0.016	0.0403
	^{214}Bi	0.6093	0.461	1.118
	^{214}Pb	0.3519	0.371	0.714
	^{214}Pb	0.2952	0.192	0.343
	^{214}Pb	0.2419	0.075	0.123
	^{226}Ra	0.1860	0.055	0.0810
	^{235}U	0.1857	0.54	0.0366

Table III

Fluxes of lunar gamma rays produced by the decay of solar-proton-produced radionuclides at the times of the Apollo 15 and 16 missions. The yield is the fraction of the disintegrations which emit that gamma ray. The elemental abundances of Table I were used.

Element	Nuclide	Energy (MeV)	Yield	Flux (photons/cm^2 min)	
				Apollo 15	Apollo 16
Mg	^{22}Na	1.2745	1.00	0.0573	0.0496
Al	^{26}Al	1.8087	0.997	0.444	0.444
	^{22}Na	1.2745	1.00	0.820	0.0710
Si	^{26}Al	1.8087	0.997	0.300	0.300
	^{22}Na	1.2745	1.00	0.0609	0.0530
Fe	^{56}Co	1.2383	0.70	0.0556	0.0187
	^{56}Co	0.8467	1.00	0.0755	0.0254
	^{54}Mn	0.8348	1.00	0.0271	0.0229

Table IV

The fluxes of gamma rays produced in the moon via neutron nonelastic-scattering reactions or the decay of GCR-produced radionuclides. The elemental abundances used for these major elements were those of Table I. The source is the reaction or radionuclide producing the gamma ray. The yield is the fraction of gamma rays with that energy produced per de-excitation of the excited level or per decay of the radionuclide.

Element	Source	Energy (MeV)	Yield	Flux (photons/cm^2 min)
O	$^{16}C(n,n\gamma)$	8.8691	0.072	0.058
	$^{16}O(n,n\gamma)$	7.1170	1.00	0.799
	$^{16}O(n,n\gamma)$	6.9172	1.00	0.728
	$^{16}O(n,n\gamma)$	6.1294	1.00	2.562
	^{16}N	6.1294	0.69	0.274
	$^{16}O(n,n\gamma)$	4.949	0.40	0.092
	$^{16}O(n,n\alpha\gamma)$	4.4383	1.00	1.200
	$^{16}O(n,n\gamma)$	4.161	0.44	0.093
	$^{16}O(n,\alpha\gamma)$	3.854	0.691	0.368
	$^{16}O(n,n\gamma)$	3.833	1.00	0.057
	$^{16}O(n,\alpha\gamma)$	3.6842	1.00	0.684
	$^{16}O(n,\alpha\gamma)$	3.086	1.00	0.280
	$^{16}O(n,n\gamma)$	2.7408	0.76	0.355
	$^{16}O(n,n\gamma)$	1.753	0.126	0.045
Mg	$^{24}Mg(n,n\gamma)$	4.238	0.76	0.107
	$^{24}Mg(n,n\gamma)$	3.8671	0.983	0.060
	^{24}Na	2.7539	0.9995	0.106
	$^{24}Mg(n,n\gamma)$	2.7539	1.00	0.091
	$^{26}Mg(n,n\gamma)$	1.8087	1.00	0.152
	$^{25}Mg(n,n\gamma)$	1.6117	1.00	0.060
	$^{24}Mg(n,n\gamma)$	1.3685	1.00	0.727
	^{24}Na	1.3686	1.00	0.069
	^{22}Na	1.2745	0.9994	0.074
	$^{26}Mg(n,n\gamma)$	1.1297	0.90	0.038

Table IV, cont.

Element	Source	Energy (MeV)	Yield	Flux (photons/cm^2 min)
Al	$^{27}Al(n,n\gamma)$	4.580	0.75	0.061
	$^{27}Al(n,n\gamma)$	4.409	0.70	0.059
	$^{27}Al(n,n\gamma)$	3.9556	0.88	0.055
	$^{27}Al(n,n\gamma)$	3.2103	0.87	0.061
	$^{27}Al(n,n\gamma)$	3.004	0.91	0.385
	$^{27}Al(n,n\gamma)$	2.981	1.00	0.120
	^{24}Na	2.7539	0.9995	0.209
	$^{27}Al(n,n\gamma)$	2.734	0.24	0.070
	$^{27}Al(n,n\gamma)$	2.2997	0.76	0.057
	$^{27}Al(n,n\gamma)$	2.2104	1.00	0.674
	^{26}Al	1.8087	0.997	0.290
	$^{27}Al(n,d\gamma)$	1.8087	1.00	0.238
	$^{27}Al(n,n\gamma)$	1.7195	0.76	0.167
	^{24}Na	1.3686	1.00	0.139
	^{22}Na	1.2745	0.9994	0.093
	$^{27}Al(n,n\gamma)$	1.0144	0.97	0.634
	$^{27}Al(n,n\gamma)$	0.8438	1.00	0.305
	^{27}Mg	0.8438	0.71	0.066
Si	$^{28}Si(n.n\gamma)$	7.4162	0.90	0.111
	$^{28}Si(n,n\gamma)$	6.8777	0.65	0.199
	$^{28}Si(n,n\gamma)$	5.6012	0.61	0.050
	$^{28}Si(n,n\gamma)$	5.1094	1.00	0.114
	$^{28}Si(n,n\gamma)$	5.0992	0.35	0.094
	$^{28}Si(n,n\gamma)$	4.4972	0.91	0.105
	$^{28}Si(n,n\gamma)$	3.2000	1.00	0.088
	$^{28}Si(n,n\gamma)$	2.8387	1.00	0.329
	^{24}Na	2.7539	0.9995	0.309
	$^{30}Si(n,n\gamma)$	2.2354	1.00	0.117
	^{26}Al	1.8087	0.997	0.306
	$^{28}Si(n,n\gamma)$	1.7788	1.00	3.223
	^{28}Al	1.7788	1.00	0.700
	^{24}Na	1.3686	1.00	0.212
	^{22}Na	1.2745	0.9994	0.152

Table IV, cont.

Energy	Source	Energy (MeV)	Yield	Flux (photons/cm^2 min)
Si	$^{29}Si(n,n\gamma)$	1.2733	1.00	0.067
Ca	$^{40}Ca(n,n\gamma)$	5.2486	0.79	0.042
	$^{40}Ca(n,n\gamma)$	3.9044	1.00	0.232
	$^{40}Ca(n,n\gamma)$	3.7366	1.00	0.346
	$^{40}Ca(n,\alpha\gamma)$	1.6112	1.00	0.106
	$^{40}Ca(n,p\gamma)$	1.1589	0.86	0.032
	$^{44}Ca(n,n\gamma)$	1.1569	1.00	0.034
	$^{40}Ca(n,p\gamma)$	0.8916	1.00	0.031
	$^{40}Ca(n,p\gamma)$	0.7705	1.00	0.101
Ti	$^{48}Ti(n,n\gamma)$	1.3117	1.00	0.037
	$^{48}Ti(n,n\gamma)$	0.9834	1.00	0.163
	$^{46}Ti(n,n\gamma)$	0.8892	1.00	0.016
	^{46}Sc	0.8892	1.00	0.013
Fe	$^{56}Fe(n,n\gamma)$	3.6019	0.69	0.040
	$^{56}Fe(n,n\gamma)$	2.601	1.00	0.061
	$^{56}Fe(n,n\gamma)$	2.5231	0.87	0.053
	$^{56}Fe(n,n\gamma)$	2.1129	1.00	0.078
	$^{56}Fe(n,n\gamma)$	1.8109	1.00	0.123
	$^{54}Fe(n,n\gamma)$	1.4077	1.00	0.061
	$^{56}Fe(n,2n\gamma)$	1.3164	1.00	0.091
	$^{56}Fe(n,n\gamma)$	1.2383	1.00	0.256
	$^{56}Fe(n,n\gamma)$	1.0380	1.00	0.041
	$^{56}Fe(n,2n\gamma)$	0.9312	1.00	0.086
	$^{56}Fe(n,n\gamma)$	0.8467	1.00	1.149
	^{54}Mn	0.8348	1.00	0.090

Table V

The fluxes of gamma rays produced in the moon via neutron nonelastic-scattering reactions or the decay of GCR-produced radionuclides. The elemental abundances used for these minor elements were those of Table I. The source is the reaction or radionuclide producing the gamma ray. The yield is the fraction of gamma rays with that energy produced per de-excitation of the excited level or per decay of the radionuclide.

Element	Source	Energy (MeV)	Yield	Flux (photons/cm^2 min)
C	$^{12}C(n,n\gamma)$	4.4383	1.00	0.00163
N	$^{14}N(n,n\gamma)$	5.1049	0.80	0.000203
	$^{14}N(n,\alpha\gamma)$	4.4441	1.00	0.000238
	$^{14}N(n,n\gamma)$	2.3127	1.00	0.000323
	$^{14}N(n,\alpha\gamma)$	2.1245	1.00	0.000165
	$^{14}N(n,n\gamma)$	1.6348	1.00	0.000176
F	$^{19}F(n,n\gamma)$	1.3569	1.00	0.00094
	$^{19}F(n,n\gamma)$	1.2358	1.00	0.00046
	$^{19}F(n,n\gamma)$	0.1971	1.00	0.00144
Na	$^{23}Na(n,n\gamma)$	2.6396	1.00	0.0064
	$^{23}Na(n,n\gamma)$	1.6364	1.00	0.0215
	^{20}F	1.6337	1.00	0.0087
	^{22}Na	1.2745	1.00	0.0120
	$^{23}Na(n,n\gamma)$	0.4399	1.00	0.0558
P	$^{31}P(n,n\gamma)$	2.2337	1.00	0.0022
	$^{31}P(n,n\gamma)$	1.2661	1.00	0.0038
S	$^{32}S(n,n\gamma)$	2.2301	1.00	0.0067
Cl	$^{35}Cl(n,n\gamma)$	1.7632	1.00	0.000100
	$^{35}Cl(n,n\gamma)$	1.2194	1.00	0.000075
Ar	$^{40}Ar(n,n\gamma)$	1.4608	1.00	0.0013
K	$^{39}K(n,n\gamma)$	2.8137	1.00	0.00354
	$^{39}K(n,n\gamma)$	2.5225	1.00	0.00275

Table V, cont.

Element	Source	Energy (MeV)	Yield	Flux (photons/cm^2 min)
Cr	$^{52}Cr(n,n\gamma)$	1.5308	1.00	0.00125
	$^{52}Cr(n,n\gamma)$	1.4342	1.00	0.0160
	$^{52}Cr(n,n\gamma)$	1.3338	1.00	0.00192
	$^{52}Cr(n,n\gamma)$	0.9356	1.00	0.00123
Mn	$^{55}Mn(n,n\gamma)$	1.5289	1.00	0.00151
	$^{55}Mn(n,n\gamma)$	1.1662	1.00	0.00186
	$^{55}Mn(n,n\gamma)$	0.8583	1.00	0.00361
	^{54}Mn	0.8348	1.00	0.00301
	$^{55}Mn(n,n\gamma)$	0.1260	1.00	0.00330
Ni	$^{58}Ni(n,n\gamma)$	1.4544	1.00	0.00260
	$^{60}Ni(n,n\gamma)$	1.3325	1.00	0.00169
	^{58}Co	0.8106	1.00	0.00105
Sr	$^{88}Sr(n,n\gamma)$	1.8360	1.00	0.0019
Y	^{88}Y	1.8360	0.994	0.00020
	$^{89}Y(n,n\gamma)$	1.7445	1.00	0.00023
	$^{89}Y(n,n\gamma)$	1.5074	1.00	0.00024
	$^{89}Y(n,n\gamma)$	0.9092	1.00	0.00019
Zr	$^{90}Zr(n,n\gamma)$	2.1865	1.00	0.00090
	$^{92}Zr(n,n\gamma)$	0.9345	1.00	0.00050
	$^{94}Zr(n,n\gamma)$	0.9182	1.00	0.00049
	^{89}Zr	0.9092	1.00	0.00043
Ba	$^{138}Ba(n,n\gamma)$	1.4359	1.00	0.00147

Table VI

The fluxes of gamma rays produced in the moon by spallation, (p,xγ), reactions. Table I elemental abundances are used. The source is the excited nuclide made by reactions of GCR particles with the element.

Element	Source	Energy (MeV)	Flux (photons/cm^2 min)
Mg	$^{20}Ne^*$	1.6337	0.07
Al	$^{23}Na^*$	1.6364	0.07
	$^{20}Ne^*$	1.6337	0.11
	$^{24}Mg^*$	1.3686	0.15
Si	$^{27}Al^*$	2.2104	0.10
	$^{20}Ne^*$	1.6337	0.20
	$^{24}Mg^*$	1.3686	0.52
	$^{27}Al^*$	1.0144	0.10
Ca	$^{39}K^*$	2.8137	0.06
	$^{39}Ca^*$	2.793	0.11
	$^{32}S^*$	2.2301	0.05
	$^{36}Ar^*$	1.9704	0.15
Fe	$^{52}Cr^*$	1.4342	0.05

Table VII

The fluxes of gamma rays produced in the moon by neutron-capture reactions with the major elements. (See Table I for the elemental abundances used.) The yield is the fraction of captures by the element which produces the gamma ray. The source indicates the isotope in which the neutron was captured or the radionuclide, produced by neutron capture, which decayed to produce the gamma ray.

Element	Source	Energy (MeV)	Yield	Flux (photons/cm^2 min)
Mg	$^{24}Mg(n,\gamma)$	3.918	0.48	0.0201
	$^{24}Mg(n,\gamma)$	2.8285	0.36	0.0117
Al	$^{27}Al(n,\gamma)$	7.724	0.30	0.169
	$^{27}Al(n,\gamma)$	7.694	0.045	0.025
	$^{27}Al(n,\gamma)$	4.735	0.057	0.025
	$^{27}Al(n,\gamma)$	4.260	0.06	0.024
	$^{27}Al(n,\gamma)$	4.134	0.065	0.026
	$^{27}Al(n,\gamma)$	3.0345	0.08	0.025
	$^{27}Al(n,\gamma)$	2.960	0.09	0.027
	^{28}Al	1.7788	1.00	0.205
Si	$^{28}Si(n,\gamma)$	7.200	0.08	0.053
	$^{28}Si(n,\gamma)$	6.381	0.13	0.081
	$^{28}Si(n,\gamma)$	4.934	0.61	0.330
	$^{28}Si(n,\gamma)$	3.5395	0.66	0.281
	$^{28}Si(n,\gamma)$	2.0931	0.20	0.057
	$^{28}Si(n,\gamma)$	1.2733	0.19	0.037
Ca	$^{40}Ca(n,\gamma)$	6.420	0.40	0.236
	$^{40}Ca(n,\gamma)$	5.9005	0.07	0.039
	$^{40}Ca(n,\gamma)$	4.419	0.18	0.086
	$^{40}Ca(n,\gamma)$	2.0015	0.18	0.046
	$^{40}Ca(n,\gamma)$	1.9427	0.80	0.201

Table VII, cont.

Element	Source	Energy (MeV)	Yield	Flux (photons/cm^2 min)
Ti	$^{48}Ti(n,\gamma)$	6.7615	0.40	0.404
	$^{48}Ti(n,\gamma)$	6.557	0.04	0.040
	$^{48}Ti(n,\gamma)$	6.419	0.28	0.275
	$^{48}Ti(n,\gamma)$	4.882	0.05	0.042
	$^{48}Ti(n,\gamma)$	1.7620	0.045	0.017
	$^{48}Ti(n,\gamma)$	1.5853	0.09	0.032
	$^{48}Ti(n,\gamma)$	1.4983	0.04	0.014
	$^{48}Ti(n,\gamma)$	1.3813	0.82	0.264
	$^{48}Ti(n,\gamma)$	0.3419	0.38	0.048
Fe	$^{54}Fe(n,\gamma)$	9.299	0.034	0.091
	$^{56}Fe(n,\gamma)$	7.6457	0.22	0.542
	$^{56}Fe(n,\gamma)$	7.6313	0.24	0.591
	$^{56}Fe(n,\gamma)$	7.279	0.05	0.121
	$^{56}Fe(n,\gamma)$	6.019	0.08	0.174
	$^{56}Fe(n,\gamma)$	5.921	0.08	0.173
	$^{56}Fe(n,\gamma)$	4.810	0.018	0.035
	$^{56}Fe(n,\gamma)$	4.2185	0.04	0.070
	$^{56}Fe(n,\gamma)$	1.725	0.09	0.079
	$^{56}Fe(n,\gamma)$	1.6126	0.07	0.059
	$^{56}Fe(n,\gamma)$	0.6921	0.08	0.036

Table VIII

The fluxes of gamma rays produced in the moon by neutron-capture reactions with minor or trace elements. (See Table I for the elemental abundances used.) The yield is the fraction of captures by the element which produces the gamma ray. The source indicates the isotope in which the neutron was captured or the radionuclide, produced by neutron capture, which decayed to produce the gamma ray.

Element	Source	Energy (MeV)	Yield	Flux (photons/cm^2 min)
H	$^{1}H(n,\gamma)$	2.2233	1.00	0.00342
N	$^{14}N(n,\gamma)$	10.8295	0.135	0.000050
	$^{14}N(n,\gamma)$	6.3225	0.184	0.000054
	$^{14}N(n,\gamma)$	5.5334	0.185	0.000050
	$^{14}N(n,\gamma)$	5.298	0.217	0.000057
	$^{14}N(n,\gamma)$	5.2693	0.311	0.000082
Na	$^{23}Na(n,\gamma)$	6.395	0.20	0.0089
	^{24}Na	2.7539	0.9995	0.0248
	^{24}Na	1.3686	1.00	0.0144
	$^{23}Na(n,\gamma)$	0.4723	1.00	0.0069
S	$^{32}S(n,\gamma)$	5.424	0.55	0.0031
	$^{32}S(n,\gamma)$	2.379	0.40	0.0012
Cl	$^{35}Cl(n,\gamma)$	7.791	0.09	0.00102
	$^{35}Cl(n,\gamma)$	7.415	0.11	0.00122
	$^{35}Cl(n,\gamma)$	6.621	0.09	0.00094
	$^{35}Cl(n,\gamma)$	6.111	0.21	0.00211
	$^{35}Cl(n,\gamma)$	1.951	0.20	0.00088
K	$^{39}K(n,\gamma)$	7.770	0.07	0.0027
	$^{39}K(n,\gamma)$	5.7525	0.07	0.0023
	$^{39}K(n,\gamma)$	5.697	0.07	0.0023
	$^{39}K(n,\gamma)$	5.381	0.09	0.0029
	$^{39}K(n,\gamma)$	0.7705	0.58	0.0044

Table VIII, cont.

Element	Source	Energy (MeV)	Yield	Flux (photons/cm^2 min)
Cr	$^{53}Cr(n,\gamma)$	9.719	0.10	0.0040
	$^{53}Cr(n,\gamma)$	8.884	0.24	0.0091
	$^{52}Cr(n,\gamma)$	7.939	0.11	0.0040
Mn	$^{55}Mn(n,\gamma)$	7.244	0.10	0.0113
	$^{55}Mn(n,\gamma)$	7.058	0.09	0.0101
	^{56}Mn	1.8109	0.29	0.0125
	^{56}Mn	0.8467	0.988	0.024
Ni	$^{58}Ni(n,\gamma)$	8.999	0.37	0.0072
	$^{58}Ni(n,\gamma)$	8.534	0.18	0.0034
Sr	$^{87}Sr(n,\gamma)$	1.8360	0.45	0.00025
Y	$^{89}Y(n,\gamma)$	6.080	0.4	0.00018
Nd	$^{143}Nd(n,\gamma)$	0.697	0.65	0.00042
Sm	$^{149}Sm(n,\gamma)$	0.4395	0.4	0.0095
	$^{149}Sm(n,\gamma)$	0.3340	0.7	0.014
Eu	^{152g}Eu	1.409	0.15	0.0024
	^{152g}Eu	1.113	0.09	0.0012
Gd	$^{157}Gd(n,\gamma)$	6.747	0.02	0.009
	$Gd(n,\gamma)$	1.187	0.11	0.014
	$^{157}Gd(n,\gamma)$	0.945	0.07	0.007
	$^{157}Gd(n,\gamma)$	0.182	0.22	0.008

Figure Caption

Fig. 1. The gamma-ray fluxes calculated as escaping from the moon for the average lunar chemical composition of Table I are shown as a function of their energies. The more intense gamma rays are labeled by the element or radionuclide producing them.

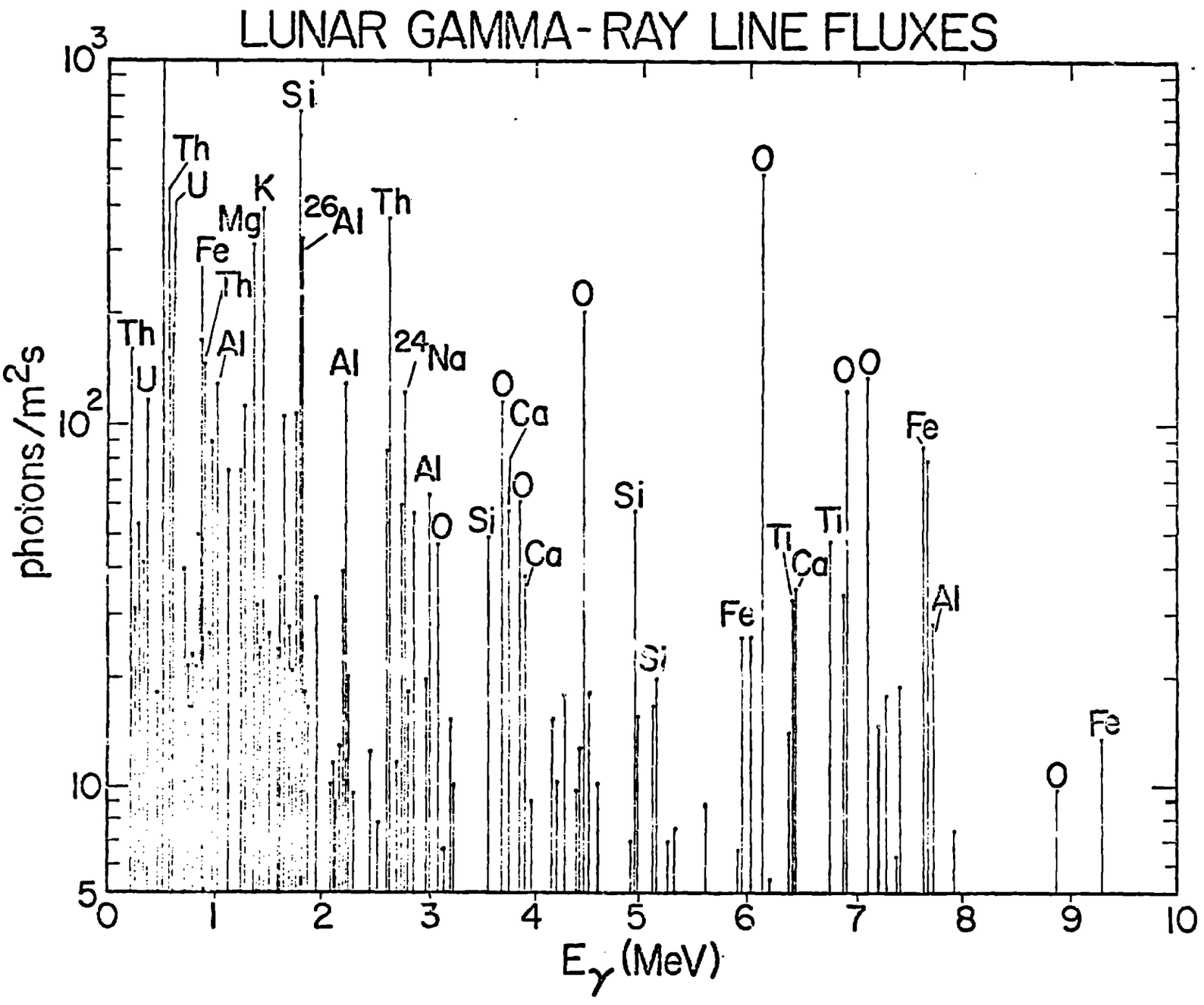
LUNAR GAMMA-RAY LINE FLUXES
photons/m²s
10^3
10^2
10
5
0
1
2
3
4
5
6
7
8
9
10
E_γ (MeV)
Th
U
K
Mg
Fe
Th
Al
Si
^{26}Al
Th
Al
^{24}Na
Al
O
Si
O
Ca
O
Ca
O
Si
Si
O
Fe
O
Ti
Ti
Ca
O
O
Fe
Al
O
Fe

Fig. 1